International Journal of Engineering & Technology, 7 (4.15) (2018) 405-408

International Journal of Engineering & Technology

Website: www.sciencepubco.com/index.php/IJET

Research paper

Relationship between the voltage applied to MZM arms and the generation of optical frequency comb

Yousif I. Hammadi[1]*, Tahreer S. Mansour[1]

[1]*Laser Institute for Postgraduate Studies, University of Baghdad, Iraq*
**Corresponding author E-mail: yousif.ibrahim.hammadi@gmail.com*

Abstract

In this study, an optical frequency comb source (OFCS) based on a dual-drive Mach–Zehnder modulator (MZM) is constructed and theoretically demonstrated. A mathematical model of the constructed OFCS is then built to investigate the effect of the peak-to-peak radio frequency (RF) signals applied to the MZM arms on the generated optical frequency comb (OFC) lines at the MZM output. A dual-drive MZM, a continuous wave laser source, and an RF signal source are included in the OFCS. The chirp parameter can be controlled and 64 comb lines generated at a comb spacing of 25 GHz by regulating voltages applied to the MZM arms. The developed OFCS is relatively simple but valuable. The generated OFC lines can be used for high data-rate transmission.

Keywords: *Optical frequency comb source, Dual-drive MZM, Comb spacing, Chirp parameter, Peak-to-peak voltage.*

1. Introduction

Optical frequency comb (OFC) generation has elicited considerable attention due its widespread applications, including those in metrology, spectroscopy, optical communications, and terahertz wireless technology [1– 4]. High-quality OFC lines have recently exhibited the potential for clear communications and for providing a wide range of optical carriers for dense wavelength division multiplexing and optical orthogonal frequency-division multiplexing [5]. Frequency comb lines are inherently equally spaced. Furthermore, the efficient mitigation of fiber nonlinearity during transmission can be facilitated by mutual carrier coherence from the same source [6,7].

To date, numerous approaches have been proposed for generating OFC. For example, a mode-locked laser can be used to generate OFC [8]. Such laser requires a complicated feedback loop to ensure a stable operation, and the pacing of comb lines is difficult to tune. Nonlinear effects in a nonlinear medium can also be used to generate OFC; these effects include stimulated Brillouin scattering and four-wave mixing effects [9]. However, these methods require complicated structures and high-power optical amplifiers. Another effective approach for OFC generation is the external modulation of continuous wave (CW) light; this approach provides stable operation, high flexibility, and easily tunable comb frequency spacing [10]. In [11], the researchers controlled the DC bias voltage applied to the Mach–Zehnder modulator (MZM) arms with constant radio frequency (RF) signal amplitude to generate 17 comb lines with a spacing of 12.5 GHz from a single MZM. Similarly, nine comb lines were generated within a power fluctuation of 1.2 dB from a dual-drive MZM [12]. Meanwhile, 57 comb lines with a comb spacing of 1 GHz were generated using Gaussian pulse with a width of 0.2 T at full width at half maximum as an electrical driving signal for a single MZM with a chirp factor of 6. However, generating a Gaussian pulse in the electrical domain is limited by electrical processing [13].

This paper reports the generation of OFC using a dual-drive MZM. The remainder of this paper is organized as follows. The operating principle and mathematical modeling of the constructed OFC source (OFCS) are described in Section 2. The simulation results are presented in Section 3. The effect of the voltages applied to the MZM arms on the resulting comb lines is also investigated in this section. Finally, the conclusions drawn from the study are provided in Section 4.

2. Operating principle and mathematical modeling

The schematic of the OFCS based on MZM is shown in Figure 1. The OFCS consists of a dual-drive lithium niobate ($LiNbO_3$) MZM, a CW laser, and an RF signal source. The CW laser is modulated by RF signals, and OFC lines are generated at the MZM output. These lines are visualized using an optical spectrum analyzer.

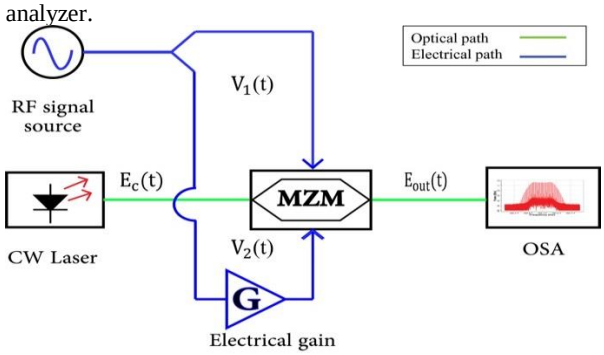

Fig.1 Schematic of the optical frequency comb source

The MZM has two arms and dual electrodes (i.e., separate DC and RF). Such electrode configuration enables separate control of DC and RF signals to regulate the operating point and chirp effect. The MZM uses RF and inverted RF signals to generate intensity modulation. Electrical driving voltages are applied to both arms of

the MZM, and phase changes of ±л/2 occur in the arms. Subsequently, RF-driven signals with different phase shifts are applied to the two arms, and different DC voltages are used to bias these arms. The voltage applied to the electrode is changed to control the optical phase in each arm. By disregarding the insertion loss with an equal power division between the two arms of the MZM, the optical field at the MZM output is expressed as [14]

$$E_{out}(t) = \frac{E_c(t)}{2}\left\{e^{j\frac{\pi V_1(t)}{V_\pi}} + e^{j\frac{\pi V_2(t)}{V_\pi}}\right\} \quad (1)$$

where
Vπ is the half-wave voltage of the MZM that is required to produce a phase shift of 180°.

$E_c(t)$ denotes the input optical field of the MZM, which is expressed as

$$E_c(t) = \sqrt{p_c}e^{j2\pi f_c t} \quad (2)$$

where p_c and f_c indicate the power and center frequency of the optical carrier, respectively.

$V_1(t)$ and $V_2(t)$ represent the voltages applied to the two arms of the MZM. These voltages are defined using the following equations:

$$V_1(t) = V_{dc1} + \frac{V_{pp1}}{2}\sin(2\pi f_e t) \quad (3)$$

$$V_2(t) = V_{dc2} + \frac{V_{pp2}}{2}\sin(2\pi f_e t) \quad (4)$$

where V_{dc1} and V_{dc2} represent the DC bias voltages applied to the MZM arms, V_{pp1} and V_{pp2} denote the peak-to-peak RF signals applied to the MZM arms, and f_e indicates the frequency of the RF signals. When Equations (3) and (4) are substituted into Equation (1), the optical field at the MZM output becomes

$$E_{out}(t) = \frac{E_c(t)}{2}\left\{e^{j\frac{\pi V_{dc1}}{V_\pi}+j\frac{\pi V_{pp1}}{2V_\pi}\sin(2\pi f_e t)} + e^{j\frac{\pi V_{dc2}}{V_\pi}+j\frac{\pi V_{pp2}}{2V_\pi}\sin(2\pi f_e t)}\right\} \quad (5)$$

Equation (5) can be simplified as

$$E_{out}(t) = \frac{\sqrt{p_c}}{2}e^{j2\pi f_c t}\left\{e^{j\theta_1+j m_1\sin(2\pi f_e t)} + e^{j\theta_2+j m_2\sin(2\pi f_e t)}\right\} \quad (6)$$

where $\theta_1 = \pi V_{dc1}/V_\pi$ and $\theta_2 = \theta_2 = \pi V_{dc2}/V_\pi$ are the static phase shifts induced by the DC biases , whereas $m_1 = \pi V_{pp1}/2V_\pi$ and $m_2 = \pi V_{pp2}/2V_\pi$ are the phase shifts induced by the RF signals.
Based on Jacobi-Anger expansion, equation (6) can be written as

$$E_{out}(t) = \frac{\sqrt{p_c}}{2}\sum_{n=-\infty}^{\infty}\left[J_n(m_1)e^{j\theta_1} + J_n(m_2)e^{j\theta_2}\right]e^{j(2\pi(f_c+nf_e)t)} \quad (7)$$

where J_n is the n^{th} order of the first kind of Bessel function.
As shown in Equation (7), the center frequency of the generated OFC is determined by the center frequency (f_c) of the laser source. Furthermore, the frequency (f_e) of the RF signal governs comb frequency spacing. The number of the generated OFC lines is determined by m_1, m_2, θ_1, and θ_2 in Equation (7). That is, if the number of the generated OFC lines is controlled by the peak-to-peak RF signals, then DC bias voltages are applied to the MZM arms. Accordingly, various results can be obtained when different values of m_1, m_2, θ_1, and θ_2 are adjusted in Equation (7). Chirping may occur when driving RF signals are controlled. Therefore, the chirping effect should be considered.
The change in phase of the output light with time causes chirping in the optical signal in the optical intensity modulator. Chirping enables increasing or decreasing the frequency of the optical signal when the driving signal is varied. The dual-electrode modulator allows the drive voltages to be varied independently; thus, a dual-electrode MZM that enables access to both electrodes can be adopted to achieve a variable chirp parameter. The chirping behavior of MZM is characterized by the chirp parameter (α_c), which is given by [15]

$$\alpha_c = \frac{V_{pp1} + V_{pp2}}{V_{pp1} - V_{pp2}} \quad (8)$$

Equation (8) clearly shows that the chirp parameter can be related to the relative amplitude and sign of the driving RF signals for each electrode. Therefore, the chirp parameter can be controlled by modulating the peak-to-peak RF signals applied to the MZM arms.
The generated OFC from the MZM is investigated under three cases depending on the analysis presented in Equations (7) and (8).
An identical phase shift is obtained in the two arms of the MZM in the case where $V_2(t) = V_1(t)$; that is, $m_2 = m_1$ and $\theta_2 = \theta_1$. Then, phase modulation is achieved. In particular, the MZM operates as a single-phase modulator in push–push mode. From Equation (7), the optical field at the MZM output is given by

$$E_{out}(t) = \sqrt{p_c}\,e^{j\theta_1}\sum_{n=-\infty}^{\infty}J_n(m_1)\;e^{j(2\pi(f_c+nf_e)t)} \quad (9)$$

Meanwhile, an opposite phase shift is induced in the two arms of the MZM in the case where $V_2(t) = -V_1(t)$; that is, $m_2 = -m_1$ and $\theta_2 = -\theta_1$. Then, intensity modulation can be obtained. In particular, the MZM operates in push–pull mode. From Equation (7), the optical field at the MZM output is given by

$$E_{out}(t) = \frac{\sqrt{p_c}}{2}\sum_{n=-\infty}^{\infty}\left[J_n(m_1)e^{j\theta_1} + J_n(-m_1)e^{-j\theta_1}\right]e^{j(2\pi(f_c+nf_e)t)} \quad (10)$$

When the values of n are odd, $J_n(m_1) = -J_n(-m_1)$. When the values of n are even, $J_n(m_1) = J_n(-m_1)$. Accordingly, Equation (10) becomes

$$E_{out}(t) = \frac{\sqrt{p_c}}{2}\sum_{n=-\infty}^{\infty}J_n(m_1)\left[e^{j\theta_1} + e^{-j\theta_1} \times (-1)^n\right]e^{j(2\pi(f_c+nf_e)t)} \quad (11)$$

Given that $-1 = e^{j\pi}$, Equation (11) is transformed to

$$E_{out}(t) = \frac{\sqrt{p_c}}{2}\sum_{n=-\infty}^{\infty}J_n(m_1)\left[e^{j\theta_1} + e^{j(n\pi-\theta_1)}\right]e^{j(2\pi(f_c+nf_e)t)} \quad (12)$$

The MZM operates in an asymmetric mode when the input signals in both arms of the MZM differ, such that $V_2(t) = -kV_1(t)$. From Equation (7), the optical field at the MZM output is given by

$$E_{out}(t) = \frac{\sqrt{p_c}}{2} \sum_{n=-\infty}^{\infty} \left[J_n(m_1) e^{j\theta_1} + J_n(-km_1) e^{-jk\theta_1} \right] e^{j(2\pi(f_c + nf_e)t)} \quad (13)$$

where K is the difference voltage factor between the two arms of the MZM.

3. Simulation results

Computer simulations have been conducted using the Optisystem software package to examine the performance of the constructed OFCS, as shown in Figure 1. The simulated parameters related to the components used in the OFCS setup are shown in Table (1). A CW laser with an optical spectrum, shown in Figure 2(a), is launched to the MZM. The MZM operates in quadrature point. Consequently, the MZM is placed at the midpoint of the optical response curve by the bias voltage. Hence, the intensity is at 50% of its peak value.

Table 1 Parameters values of the simulated system.

Component	Parameter	Value
RF signal source	f_e	25 GHz
CW laser	p_c	20 dBm
	f_c	193.1 THz
	Δf	1 MHz
MZM	E_r	100 dB
	V_{dc}	2 V

As shown in Figure 2(b), the MZM operates in push–push mode and 15 comb lines at a comb spacing of 25 GHz are generated by adjusting the peak-to-peak voltages to $V_{pp1} = V_{pp2} = 2\,V$. The same voltages (but with an opposite sign) are applied to the MZM arms when the peak-to-peak voltages are set to $V_{pp1} = 2\,V$ and $V_{pp2} = -2\,V$. Accordingly, the MZM operates in push–pull mode and 40 comb lines are generated at a comb spacing of 25 GHz, as shown in Figure 2(c). From Equation (8), the chirp parameter is zero in this case. Meanwhile, 48 comb lines at a comb spacing of 25 GHz are generated in the case where the peak-to-peak voltages are set to $V_{pp1} = 1\,V$ and $V_{pp2} = -3\,V$, as depicted in Figure 2(d). The MZM operates in an asymmetric mode in this case, and the chirp parameter is −0.5 based on Equation (8). When the peak-to-peak voltages are set to be V_{pp1}=6 V and V_{pp2}=4 V, 64 comb lines with a comb spacing of 25 GHz are generated, as illustrated in Figure 2(e). The chirp parameter is 5 in this case based on Equation (8)

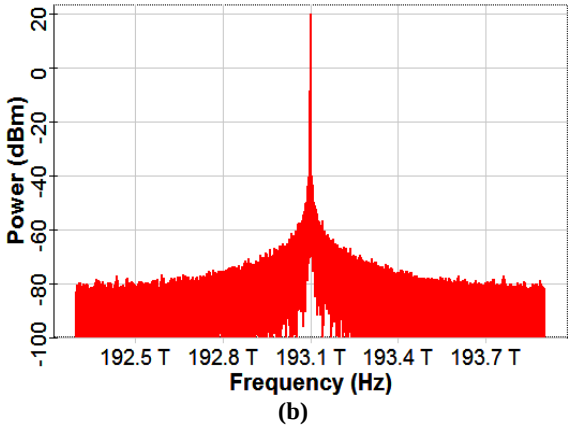

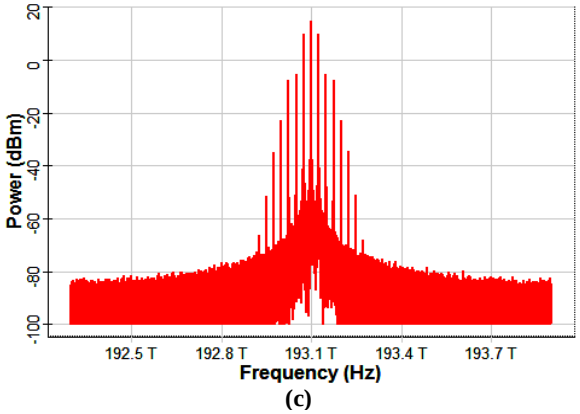

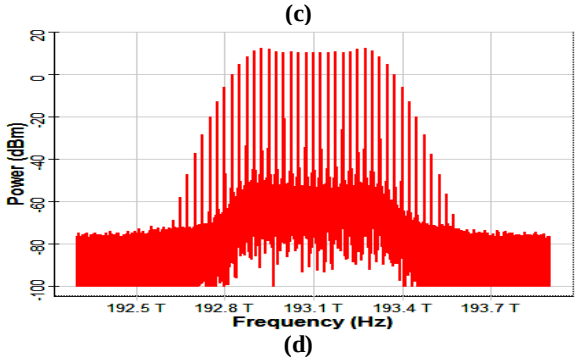

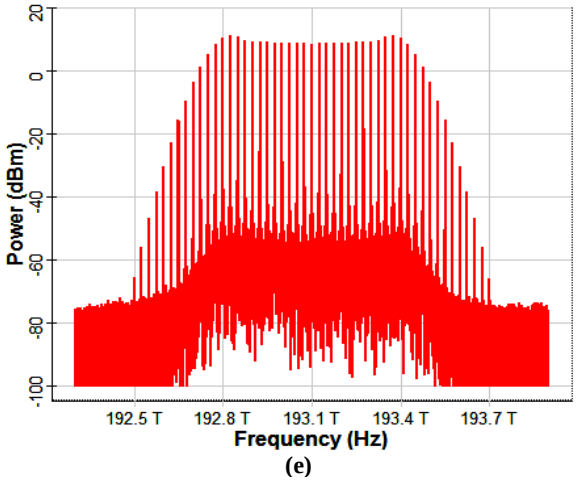

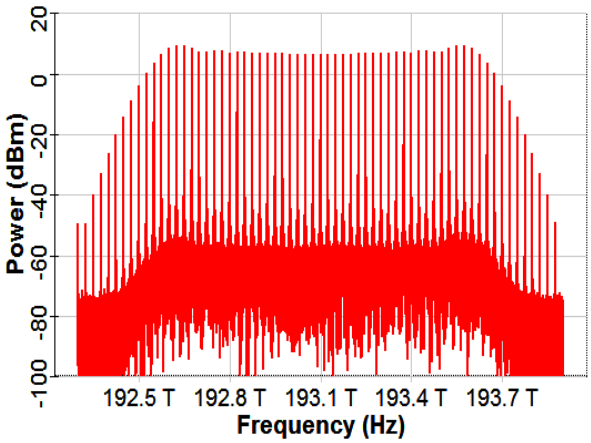

Fig. 2 Generated OFC using MZM comb source: (a) $V_2 = V_1$, (b) $V_2 = -V_1$, (c) $V_2 = -0.333V_1$,and (d) $V_2 = 0.666V_1$

4. Conclusion

An optical frequency comb source based on a dual-drive MZM was constructed, modeled, and simulated in this study. The following conclusion can be drawn from the mathematical

modeling in Section 2 and the simulated results in Section 3. First, the chirp parameter can be tuned to be positive, zero, or negative by controlling the voltage swings and the voltages at the two arms of the MZM. Second, numerous comb lines can be generated when the operating mode of the MZM is asymmetric. Third, the number of comb lines increases when the chirp parameter is increased. On the basis of the simulated results, the constructed OFCS produces 15 comb lines when the peak-to-peak RF signals applied to the MZM arms are equal. It generates 40 comb lines when the peak-to-peak RF signals applied to the MZM arms are equal but with opposite signs and 48 comb lines when the peak-to-peak RF signals are different and have opposite signs.

References

[1] T. Udem, R. Holzwarth, and T. W. Hänsch, "Optical frequency metrology," Nature, vol. 416, no. 6877, pp. 233–237, 2002.

[2] F. C. Cruz, "Optical frequency combs generated by four-wave mixing in optical fibers for astrophysical spectrometer calibration and metrology," Opt. Exp., vol. 16, no. 17, pp. 13267-13275, 2008

A. Cingöz, D. C. Yost, T. K. Allison, A. Ruehl, M. E. Fermann, I. Hartl, and J. Ye, "Direct frequency comb spectroscopy in the extreme ultraviolet," Nature, vol. 482, no. 7383, pp. 68–71, 2012.

[3] S. Bennett, B. Cai, E. Burr, O. Gough, and A. J. Seeds, "1.8-THz bandwidth, zero-frequency error, tunable optical comb generator for DWDM applications," IEEE Photonics Technol. Lett. 11(5), 551–553, 1999.

[4] Yu, S., Bao, F., & Hu, H. (2018). "Broadband optical frequency comb generation with flexible frequency spacing and center wavelength". IEEE Photonics Journal, 10(2), 1-7..

[5] Fulop, A., Mazur, M., Eriksson, T. A., Andrekson, P. A., Wang, P. H., Xuan, Y., ... & Weiner, A. M. (2016, June). "Long-haul coherent transmission using a silicon nitride microresonator-based frequency comb as WDM"

[6] Temprana, E., Myslivets, E., Kuo, B. P., Liu, L., Ataie, V., Alic, N., & Radic, S. (2015) "Overcoming Kerr-induced capacity limit in optical fiber transmission. Science", 348(6242), 1445-1448.

[7] Endo, M., Shoji, T. D., & Schibli, T. R. (2018). "Ultralow Noise Optical Frequency Combs." IEEE Journal of Selected Topics in Quantum Electronics, 24(5), 1-13..

[8] W. Liang, D. Eliyahu, V. S. Ilchenko, A. A. Savchenkov, D. Seidel, L. Maleki, and A. B. Matsko, "High spectral purity Kerr frequency comb radio frequency photonic oscillator," Nature Communications, vol. 6, no. 7957, pp. 1–8, 2015

[9] Gürel, K., Hakobyan, S., Wittwer, V. J., Schilt, S., & Südmeyer, T. (2018). "Frequency comb stabilization of ultrafast lasers by opto-optical modulation of semiconductors". IEEE Journal of Selected Topics in Quantum Electronics, 24(5), 1-9.

[10] Yamamoto, T., Hitomi, K., Kobayashi, W., & Yasaka, H. (2013). "Optical frequency comb block generation by using semiconductor Mach–Zehnder modulator". IEEE Photonics Technology Letters, 25(1), 40-42

[11] Mishra, A. K., Schmogrow, R., Tomkos, I., Hillerkuss, D., Koos, C., Freude, W., & Leuthold, J.,"Flexible RF-based comb generator". IEEE Photon. Technol. Lett., 25(7), 701-704, 2013

[12] Hmood, J. K., & Harun, S. W. (2018). "Broadband optical frequency comb generator based on driving N-cascaded modulators by Gaussian-shaped waveform. Optical Fiber Technology", 42, 75-83

[13] Agrawal, G. P. (2012). "Fiber-optic communication systems" (Vol. 222). John Wiley & Sons

[14] Smith, Graham H., Dalma Novak, and Zaheer Ahmed. "Overcoming chromatic-dispersion effects in fiber-wireless systems incorporating external modulators" IEEE transactions on microwave theory and techniques 45, no. 8 ,1410-1415, 1997